Crisis route to chaos in semiconductor lasers subjected to external optical feedback

Michael J. Wishon,[1,2] Alexandre Locquet,[1,2,*] C. Y. Chang,[1,3] D. Choi,[1,2] and D. S. Citrin[1,2]

[1]*UMI 2958 Georgia Tech-CNRS, Georgia Tech Lorraine, 2 Rue Marconi, 57070 Metz, France*
[2]*School of Electrical and Computer Engineering, Georgia Institute of Technology, Atlanta, Georgia, 30332-0250, USA*
[3]*School of Physics, Georgia Institute of Technology, Atlanta, Georgia, 30332-0250, USA*

Semiconductor lasers subjected to optical feedback have been intensively used as archetypal testbeds for high-speed (sub-ns) and high-dimensional nonlinear dynamics. By simultaneously extracting all the dynamical variables, we demonstrate that for larger current, the commonly named "quasiperiodic" route is in fact based on mixed external-cavity solutions that lock the oscillation frequency of the intensity, voltage, and separation in optical frequency through a mechanism involving successive rejections along the unstable manifold of an antimode. We show that chaos emerges from a crisis resulting from the inability to maintain locking as the unstable manifold becomes inaccessible.

I. INTRODUCTION

Semiconductor lasers subjected to optical self feedback from a distant reflector undergo profound modification to the coupled nonlinear dynamics of its three variables: the slowly varying amplitude of the optical field $E(t)$, the optical phase $\phi(t)$, and the carrier density in the gain medium (inversion) $n(t)$. These systems have been studied for nearly 50 years [1–3], and they provide an important archetype for nonlinear time-delayed systems. Further, these systems are of intense interest for a number of high-speed applications in neuromorphic computing [4], compressive sensing [5], random number generation [6,7], secure communications [8–10], and optoelectronic oscillators [11].

It has been shown that these systems exhibit five characteristic regimes depending on feedback level η [12]. Specifically, in regime IV the dynamics bifurcate from continuous-wave CW emission on the minimum linewidth mode (MLM) to chaos. Two distinct chaotic regimes can be observed, viz. low-frequency fluctuations (LFF) and coherence collapse (CC). They manifest a loss in optical coherence and a multi-GHz broadening in the spectrums of the optical intensity, voltage, and phase. The fast-pulsing dynamics of LFF were seen experimentally in [13] confirming the theoretical mechanism related to a "Sisyphus" buildup and release associated with a chaotic itinerancy of the trajectory's progression to the maximum gain mode (MGM) [14], and it was recently resolved experimentally for all three dynamic variables in [15]. Therefore, a consensus has been reached on the chaotic trajectories and mechanisms behind the LFF regime, and we focus on CC, which also displays a multi-GHz broadening, but is preceded by other dynamics that need to be interpreted to understand the route to chaos.

In the route to chaos, there are two main frequencies whose interplay gives which route is observed. First is the relaxation-oscillation (RO) frequency f_{RO}, which results from the exchange between photons and carriers in the gain medium when either the photon or carrier population is perturbed. The other frequency is set by the feedback time delay $\tau = 2L/c$ (with L the external-cavity length and c the speed of light) associated with the round-trip time of light in the external cavity. The frequency difference between the ECMs f_{ECM} is the external-cavity free spectral range, i.e., $f_{ECM} = \tau^{-1}$. f_{ECM} is thus approximately the frequency separation between the ECM fixed-point solutions of the harmonic-oscillator-like optical modes associated with the external cavity [1]. Recently another frequency, the feedback-induced frequency shift of the optical frequency, was shown to determine which type of chaos is observed (strong or weak) [16].

The Lang and Kobayashi (LK) model, a set of coupled delay differential equations for $E(t)$, $\phi(t)$, and $n(t)$, is commonly used to describe this system [17]. LK has enjoyed considerable apparent success in predicting dynamical trends as parameters are varied. Experimental evidence for several routes to chaos have been found, viz., quasiperiodic (QP) [18], period-doubling (PD) [19], bifurcation cascade (BC) [20–22], and subharmonic routes [23]. The most commonly observed route at low current is the bifurcation cascade [20–22]. For larger current, it is the quasiperiodic route identified by Dente *et al.* [24] and by Mørk *et al.* [18] that is most common. The PD and subharmonic routes were shown to exist for restricted ranges of operating parameters. For instance, to observe the subharmonic route, it is necessary to tilt the mirror [25,26] while adjusting injection current J [23]. This route to chaos was explained numerically using multiple reflections and was termed *asymmetric* feedback caused by the mirror's tilt [25,26]. The PD route was shown to exist if the ratio of f_{RO} to f_{ECM} is an integer multiple for low $J \sim 1.6 J_{th}$ with J_{th} the threshold current at $\eta = 0$ [19]. Though as explained in Ref. [19], careful tuning of the current and cavity length, while varying feedback, is needed to observe the cascade as predicted by the LK model. We have examined this route briefly and see additional dynamics reminiscent of a bifurcation cascade

*alocquet@georgiatech-metz.fr

which complements the previously reported dynamics [19–22] and will be the subject of a future study.

In this article, we reëvaluate published experiments for the "quasiperiodic" route and explain the route using comprehensive experiments. In particular, the measurement of the real-time optical phase reveals temporally which ECMs are involved in the dynamics. We reïnterpret the route as being based on the locking between the oscillation frequencies of $I(t)$ and $V(t)$, and the separation in optical frequency between ECMs participating in the dynamics. This locking corresponds to mixed ECM solutions [27], and it does not correspond to the quasiperiodic route seen in the LK model which essentially predicts the development of quasiperiodic attractors from single ECMs [28].

II. PHASE SPACE AND EXPERIMENT

It is utile to comment here on a few basic features underlying the structure of phase space [28–34]. Fixed-point solutions of the LK model, i.e., steady-type solutions, lie on an ellipse in the n-ϕ and I-ϕ planes. Possible stable solutions of the system are given by the previously mentioned ECMs while the unstable saddle-node solutions are known as antimodes. In practice, many of the ECMs are either unstable or unreachable due to their narrow basins of attraction [32]. The ECMs are numbered positive and negative relative to the MLM on which the laser initially operates. The MLM is labeled mode 0 and ECMs of higher (lower) frequency are successively assigned positive (negative) integer indices. In other words, ECM m occurs at optical frequency $f_m = f_{MLM} + m f_{ECM}$, where f_{MLM} is the frequency of the CW output of the solitary laser with minimal feedback. The MGM occurs for the minimum value of m for which a fixed-point solution to the LK model exists [35]. In Figs. 4–7, schematic drawings (top right panel) of phase space are presented to aid in understanding which ECMs are being accessed and their relative position for the experimental data in the other two panels.

Phase space is spanned by $I(t)$, $\phi(t)$, and $n(t)$. Experimentally, we measure $I(t) \propto E(t)^2$ with a fast photodiode, $\phi(t)$ by means of heterodyning with a second frequency-stabilized laser [36], and the laser-diode terminal voltage $V(t)$, small changes in which are proportional to changes in $n(t)$ [15,21,37–39]. We thus *simultaneously* monitor $I(t)$, $\phi(t)$, and $V(t)$, and track the full dynamics in phase space, for the first time, while varying η, and fully characterize and redefine the phase-space dynamics of the route to chaos. As has been demonstrated elsewhere [11,15,37,39], the dynamics in $V(t)$ closely follow those of $I(t)$ with a phase shift due to the large role played by ROs. Thus, in this manuscript we focus on $I(t)$ and $\phi(t)$.

In the experiment (Fig. 1), two photodiodes are used to measure the dynamics, one for $I(t)$ and one for the beat signal I_{Beat} between L1 and TLS allowing for the extraction of $\phi(t)$ (Fig. 2). We use the technique for phase measurement from [36] except we use a windowing technique to isolate the phase dynamics over the requisite timescale (~0.1 ns). For lasers with external optical feedback, the route to chaos as η changes is determined by J and L *via* the interplay between f_{RO} and f_{ECM}. Here we explore the long-cavity case, $f_{ECM} < f_{RO}$, and the cavity lengths utilized were between 15 and 60 cm.
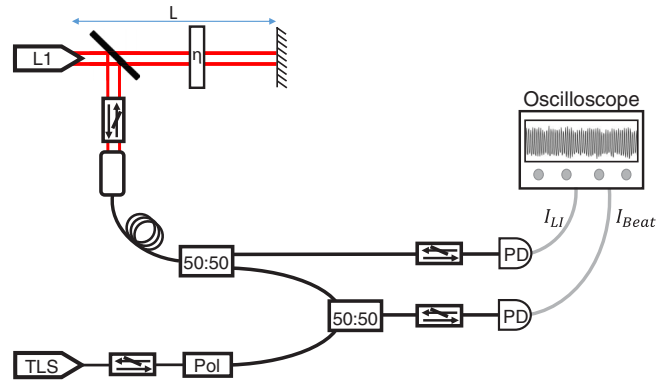

FIG. 1. Schematic diagram of the laser subjected external optical feedback and heterodyne measurement. The MQW laser under study (L1) is subjected to optical feedback from a mirror with a reflectivity of 99.97%. The feedback (η) is controlled by rotating a quarter-wave plate relative to a fixed linear polarizer. TLS is the tunable laser source for heterodyning. PD, Pol, and 50:50 stand for photodiode, polarization controller, and fiber-optic splitter or combiner, respectively.

Further, we utilized a multitude of packaged [21,38] and unpackaged [11,39] DFB lasers from different manufacturers, to understand the generality of the routes undergone depending on f_{RO} and f_{ECM}. Although several lasers were utilized in the experiment, the experimental data is from the unpackaged MQW laser in Refs. [11,39]. The Henry factor α of this laser varies from 3 to 5 depending on the pump current. The length of the laser is 600 μm and the emitting facet has an anti-reflection coating giving a residual facet reflectivity of 0.1%.

III. CRISIS ROUTE TO CHAOS

For $J \gtrsim 2J_{th}$, a universal route to chaos for multi-quantum-well (MQW) lasers with optical feedback is observed in that it ends up locking on a PD trajectory before undergoing a crisis into chaos. The variation of the dynamics as a function of η has a basic evolution of CW emission leading into closed-loop trajectories and finally CC [38,40], Fig. 3. But, as we have shown with experimental bifurcation diagrams, the initial limit cycle (LC) depends on the initial ECM [40]. In Fig. 3, we see
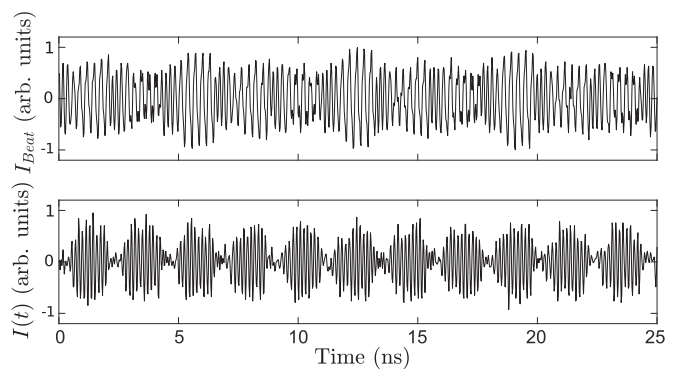

FIG. 2. Example time traces from the beat signal (I_{Beat}) and optical intensity [$I(t)$] measurements simultaneously acquired from the two photodiodes.
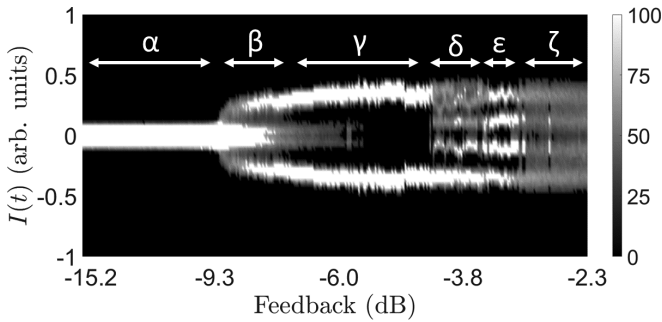
FIG. 3. A typical bifurcation diagram for high current $J > 2J_{th}$. The following progression of dynamics is observed as the optical feedback is increased, continuous-wave (α), which is followed by a quasiperiodic-like trajectory (β), limit cycles (γ), subharmonic trajectories (δ), period doubling (ϵ), and finally chaos (ζ) [21,38]. $J = 2.3J_{th}$ and $L = 30$ cm. Maximum feedback (0 dB) corresponds to $\sim 16\%$ of the optical power being coupled back onto the collimating lens.

the bifurcation diagram starting from ECM 0 which is the most common case. We believe it corresponds to what was observed in Refs. [18,28] and was proposed as a quasiperiodic route to chaos. What is seen experimentally, unless we force another initial ECM using the procedure of [40], i.e., starting from ECM 0, the fixed-point solution bifurcates into an oscillation of quasiperiodic appearance, β (around ECM +1) as seen in Fig. 4. This is quite different from the prediction of LK, that the first instability gives rise to a LC [18] and from the previous experimental interpretation [18] that this is a "noisy" LC [28]. The LK model, however, does predict the initial movement of the optical frequency toward an ECM with $m > 0$ [32]. From $\phi(t)$, Fig. 4, we see that the trajectory is characterized by a large optical frequency range. We interpret the transient CW emission portion of the trajectory as being around ECM +1, which according to Refs. [32,40] is unstable, but when $I(t)$ is characterized by fast oscillations at $\sim f_{RO}$, the optical frequency is moving between ECM 1 and ECM
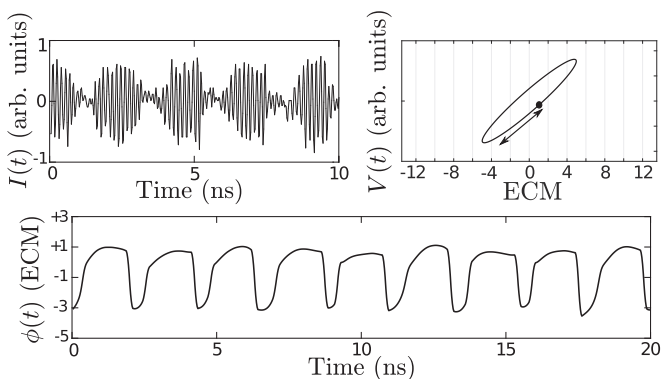

FIG. 4. The first instability, β, gives rise to a quasiperiodic-like trajectory in $I(t)$ with two distinct frequencies seen in the dynamics. The CW emission in $I(t)$ is around ECM +1, but the fast oscillation portion of $I(t)$ coincides with movement in the optical phase towards the MGM (negative ECMs). As feedback is increased the optical phase moves further and further in phase space towards negative modes (MGM) as the ellipse gets larger (not shown).
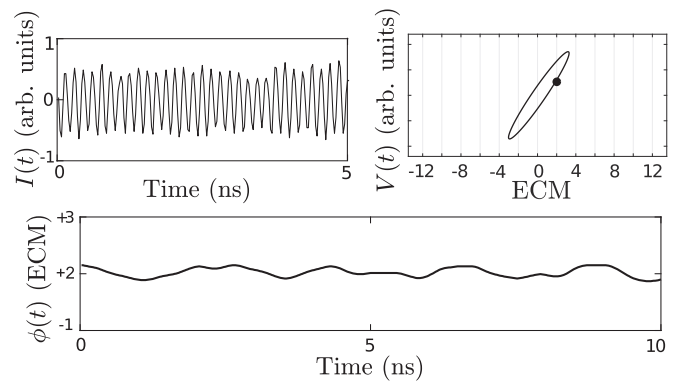

FIG. 5. An example of a limit cycle trajectory, during γ. We see a sinusoidal oscillation in the optical intensity. The optical frequency is centered around ECM +2.

-3. In addition, we observe that, with a period close to τ, the phase space trajectory suddenly moves in the direction of the MGM. It then moves back toward ECM +1, while oscillating at a frequency close to f_{RO} in $I(t)$ and $V(t)$. We suspect the oscillations and rejections are resulting from the interaction of modes and antimodes. As η is increased, the trajectory reaches out further and further from ECM +1 into phase toward negative modes (MGM) as the ellipse becomes larger. The behavior of quasiperiodic appearance is thus not resulting from excursions on a torus that has developed around an equilibrium point, as would be expected in a QP route to chaos. After the quasiperiodic-like trajectory, the optical frequency moves through a crisis to ECM +2, Fig. 5. Around this fixed-point solution, several different LCs appear in succession (γ) [38,40]. Of note, a similar sequence of LCs can be observed with the LK model [41]. The frequency of the first LC is close to f_{RO} and appears to be the multiple of f_{ECM} that is closest to f_{RO}, similar locking phenomena has also been observed in quantum dot lasers [42]. Of note, there are three distinct LCs seen around ECM +2, with each one decreasing in RF frequency by $\sim f_{ECM}$, until the final LC has a frequency of ~ 7 GHz. An example of one LC is shown in Fig. 5.

As η is increased further and the ellipse encompasses ECM -7, a bridge in phase space is opened. The bridge connects the right-hand region of $m \geqslant 0$ ECMs with the most negative ECMs proximate to the MGM. The bridge is characterized in $I(t)$ by a complex trajectory involving both LC oscillations around ECM +3 and PD trajectories between ECM 0 and -7 spanning from across phase space toward the MGM, δ. ECMs +1 and +2 have lost stability and ECMs $m > +3$ are less stable as predicted by LK in Ref. [32]. We call this regime subharmonic because the dominant frequencies in the RF spectrum sum to $\sim f_{RO}$. For example, the time series in Fig. 6 has peaks in its spectrum at $\frac{1}{4}f_{RO}$ and $\frac{3}{4}f_{RO}$. Interestingly, the system locks for a given η on different complex LCs involving an alternation between a specific number of LC oscillations and PD oscillations. In Fig. 6, $I(t)$ demonstrates a case in which there are two LC oscillations for every one PD oscillation. But, overall these trajectories are large LCs reaching from ECM +3 to the MGM. We suspect this regime results from a competition of ECMs because it is possible to have mixed ECM solutions to the LK model [27]. Noticeably, the separation
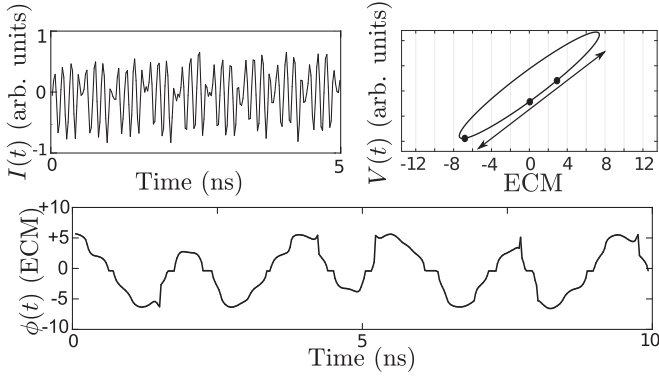
FIG. 6. An example subharmonic trajectory, during δ, with two periodic oscillations for every one PD oscillation. From the optical phase, we see periodic oscillations around $m > 0$ ECMs and PD oscillations between ECMs 0 and -7.

between ECMs 0 and -7 corresponds to 3.5 GHz $= \frac{7\,\text{GHz}}{2}$, indicating a resonance locking between the optical frequencies and half of the RF frequency of the last limit cycle. As η is subsequently increased, the trajectory spends less time around $m > 0$ ECMs and more time going between $m > 0$ ECMs and over the bridge. As new MGMs are born, we observe that the active ECMs, involved in the mixed ECM trajectory maintain the separation of 7 ECMs or 3.5 GHz by sliding from positive to negative ECMs following the MGM, i.e., the bridge 0 to -7 becomes a bridge between -1 and -8, etc., confirming the locking to 3.5 GHz of the separation between ECMs. This complex locking of LC and PD dynamics occurs until the ellipse of fixed-point solutions becomes large enough to encompass ECM -11, such that ECMs $+3$, -4, and -11 are active, from which point the dynamics of $I(t)$ are a stable period-doubled trajectory, ϵ, Fig. 7. In the period-doubled regime (Fig. 7), $\phi(t)$ switches between modes $+3$, -4, and -11, each separated by $\sim$3.5 GHz, and interestingly the dominant RF frequency of $I(t)$ and $V(t)$ are also $\sim$3.5 GHz (Fig. 8), or half the oscillation frequency of the last LC around ECM $+2$ which was 7 GHz $\approx f_{\text{ROF}} - 2 f_{\text{ECM}} = [(+3) - (-11)] f_{\text{ECM}}$. We checked that this is consistent for different f_{RO} values, by varying the current and utilizing packaged and unpackaged MQW lasers [11,21,38,39], and we observe
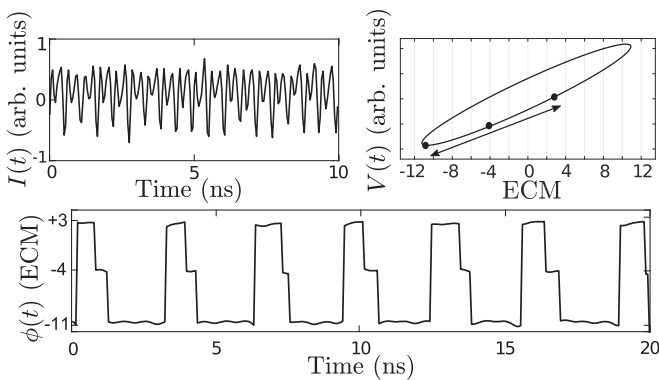

FIG. 7. Frequency halving of the final LC frequency is observed as a period-doubled trajectory, ϵ, in $I(t)$. The optical phase covers a large portion of phase space (ECMs $+3$, -4, -11).
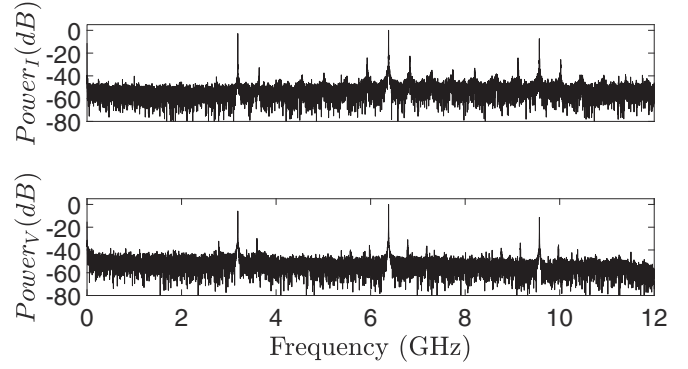

FIG. 8. An example of the RF locking between the optical intensity (top) and voltage (bottom). Both RF spectra have similar dominant frequencies with main peaks at $\sim$3.5 and 7 GHz.

the same phenomena. In Ref. [27], Pieroux *et al.* predicted similar dynamics, based on the LK model, predicated on the existence of mixed fixed-point solutions, i.e., more than one solution to the model at a time. In that theoretical study, the solutions result in periodic oscillations in, $I(t)$ and thus $V(t)$, with frequency being equal to the separation in $\phi(t)$, as is seen here, providing numerical proof for a bridge in phase space due to locking between the system's frequencies [$I(t)$, $V(t)$, and $\phi(t)$]. Also, we see a rejection after spending time around ECM -11 back to ECM $+3$, in $\phi(t)$ (Fig. 7). We suspect this is a rejection along the unstable manifold of the antimode that is nearby the MGM (ECM -11), similar to what is observed in LFF. This rejection is in fact necessary to maintain the mixed ECM solution since as η increases further the active ECMs stop moving left with the growth in the ellipse because ECM $+3$ is the most stable positive ECM. As the feedback level is increased further, the rejections along the manifold become more rare as the antimode moves further from ECM -11 until they no longer occur. At this time, a boundary crisis into chaos is observed.

For the quasiperiodic route to chaos, LK predicts the sequence of dynamics should be a bifurcation in which a LC is born, and subsequently another bifurcation leads to a quasiperiodic oscillation, possibly interrupted by windows of frequency locking, and then chaos [18]. This is remarkably different than what is seen experimentally. We observe CW emission, followed by a pseudo-quasiperiodic trajectory involving multiple ECMs, and a sequence of three stable LCs each with a discretely lower RF frequency. The final LC in the cascade has an RF frequency for intensity and voltage, which equals the separation in optical phase given by the competition of mixed ECM solutions. Finally, when locking occurs on mixed ECM solutions, the system displays PD dynamics, and undergoes a sudden transition to chaotic behavior which we interpret as a boundary crisis born from the inability to maintain locking all of the system's frequencies without a rejection along an unstable manifold.

IV. CONCLUSION

In conclusion, for larger currents and a long external cavity, we have demonstrated that a universal crisis route to chaos, previously known as the quasiperiodic route, is observed.

This crisis route involves locking the system's frequencies (phase, intensity, and carriers) through mixed external-cavity mode solutions. To confirm the generality of our discoveries, we investigated several packaged and unpackaged, MQW lasers operated at various currents giving different relaxation oscillation frequencies and the same bifurcations and crises were observed demonstrating the robustness and generality of the crisis route to chaos for MQW lasers subjected to external optical feedback.

[1] J. Ohtsubo, *Semiconductor Lasers: Stability, Instability, and Chaos*, Vol. 111 (Springer, Berlin, 2012).

[2] M. C. Soriano, J. García-Ojalvo, C. R. Mirasso, and I. Fischer, Rev. Mod. Phys. **85**, 421 (2013).

[3] A. Bogatov, P. Eliseev, L. Ivanov, A. Logginov, M. Manko, and K. Senatorov, IEEE J. Quantum Electron. **9**, 392 (1973).

[4] D. Brunner, M. C. Soriano, C. R. Mirasso, and I. Fischer, Nat. Commun. **4**, 1364 (2013).

[5] D. Rontani, D. Choi, C.-Y. Chang, A. Locquet, and D.S. Citrin, Sci. Rep. **6**, 35206 (2016).

[6] A. Uchida, K. Amano, M. Inoue, K. Hirano, S. Naito, H. Someya, I. Oowada, T. Kurashige, M. Shiki, S. Yoshimori *et al.*, Nat. Photon. **2**, 728 (2008).

[7] N. Li, B. Kim, V. Chizhevsky, A. Locquet, M. Bloch, D.S. Citrin, and W. Pan, Opt. Express **22**, 6634 (2014).

[8] A. Argyris, D. Syvridis, L. Larger, V. Annovazzi-Lodi, P. Colet, I. Fischer, J. Garcia-Ojalvo, C. R. Mirasso, L. Pesquera, and K. A. Shore, Nature **438**, 343 (2005).

[9] D. Rontani, A. Locquet, M. Sciamanna, D.S. Citrin, and S. Ortin, IEEE J. Quantum Electron. **45**, 879 (2009).

[10] A. Locquet, C. Masoller, and C. R. Mirasso, Phys. Rev. E **65**, 056205 (2002).

[11] C.-Y. Chang, M. J. Wishon, D. Choi, J. Dong, K. Merghem, A. Ramdane, F. Lelarge, A. Martinez, A. Locquet, and D.S. Citrin, IEEE J. Quantum Electron. **53**, 1 (2017).

[12] R. Tkach and A. Chraplyvy, J. Lightwave Technol. **4**, 1655 (1986).

[13] I. Fischer, G. H. M. Van Tartwijk, A. M. Levine, W. Elsässer, E. Göbel, and D. Lenstra, Phys. Rev. Lett. **76**, 220 (1996).

[14] G. Van Tartwijk, A. Levine, and D. Lenstra, IEEE J. Sel. Top. Quantum Electron. **1**, 466 (1995).

[15] D. Brunner, M. C. Soriano, X. Porte, and I. Fischer, Phys. Rev. Lett. **115**, 053901 (2015).

[16] X. Porte, M. C. Soriano, and I. Fischer, Phys. Rev. A **89**, 023822 (2014).

[17] R. Lang and K. Kobayashi, IEEE J. Quantum Electron. **16**, 347 (1980).

[18] J. Mørk, J. Mark, and B. Tromborg, Phys. Rev. Lett. **65**, 1999 (1990).

[19] J. Ye, H. Li, and J. G. McInerney, Phys. Rev. A **47**, 2249 (1993).

[20] A. Hohl and A. Gavrielides, Phys. Rev. Lett. **82**, 1148 (1999).

[21] B. Kim, N. Li, A. Locquet, and D.S. Citrin, Opt. Express **22**, 2348 (2014).

[22] B. Kim, A. Locquet, N. Li, D. Choi, and D. Citrin, IEEE J. Quantum Electron. **50**, 965 (2014).

[23] T. Mukai and K. Otsuka, Phys. Rev. Lett. **55**, 1711 (1985).

[24] G. C. Dente, P. S. Durkin, K. A. Wilson, and C. E. Moeller, IEEE J. Quantum Electron. **24**, 2441 (1988).

[25] D.-S. Seo, J.-D. Park, J. G. Mcinerney, and M. Osinski, IEEE J. Quantum Electron. **25**, 2229 (1989).

[26] J.-D. Park, D.-S. Seo, and J. G. McInerney, IEEE J. Quantum Electron. **26**, 1353 (1990).

[27] D. Pieroux, T. Erneux, B. Haegeman, K. Engelborghs, and D. Roose, Phys. Rev. Lett. **87**, 193901 (2001).

[28] J. Mork, B. Tromborg, and J. Mark, IEEE J. Quantum Electron. **28**, 93 (1992).

[29] C. Henry and R. Kazarinov, IEEE J. Quantum Electron. **22**, 294 (1986).

[30] N. Schunk and K. Petermann, IEEE J. Quantum Electron. **24**, 1242 (1988).

[31] A. Ritter and H. Haug, J. Opt. Soc. Am. **10**, 130 (1993).

[32] C. Masoller and N. B. Abraham, Phys. Rev. A **57**, 1313 (1998).

[33] G. Acket, D. Lenstra, A. D. Boef, and B. Verbeek, IEEE J. Quantum Electron. **20**, 1163 (1984).

[34] T. Sano, Phys. Rev. A **50**, 2719 (1994).

[35] A. M. Levine, G. H. M. Van Tartwijk, D. Lenstra, and T. Erneux, Phys. Rev. A **52**, R3436(R) (1995).

[36] D. Brunner, X. Porte, M. C. Soriano, and I. Fischer, Sci. Rep. **2**, 732 (2012).

[37] R. Kazarinov and R. Suris, J. Exp. Theor. Phys. **66**, 1067 (1974).

[38] B. Kim, A. Locquet, D. Choi, and D.S. Citrin, Phys. Rev. A **91**, 061802 (2015).

[39] C. Chang, D. Choi, A. Locquet, M. J. Wishon, K. Merghem, A. Ramdane, F. Lelarge, A. Martinez, and D.S. Citrin, Appl. Phys. Lett. **108**, 191109 (2016).

[40] A. Locquet, B. Kim, D. Choi, N. Li, and D.S. Citrin, Phys. Rev. A **95**, 023801 (2017).

[41] P. M. Alsing, V. Kovanis, A. Gavrielides, and T. Erneux, Phys. Rev. A **53**, 4429 (1996).

[42] B. Tykalewicz, D. Goulding, S. P. Hegarty, G. Huyet, T. Erneux, B. Kelleher, and E. A. Viktorov, Opt. Express **24**, 4239 (2016).